JCTC Journal of Chemical Theory and Computation

Formation of Interconnected Aggregates in Aqueous Dicationic Ionic Liquid Solutions

B. L. Bhargava*,†,‡ and Michael L. Klein†

Institute for Computational Molecular Science and Department of Chemistry, Temple University, 1900 N. 12th Street, Philadelphia, Pennsylvania 19122, and The Laboratory for Research on the Structure of Matter, University of Pennsylvania, 3231 Walnut Street, Philadelphia, Pennsylvania 19104-6202

Received December 15, 2009

Abstract: The structure and organization in an aqueous solution of a gemini surfactant, the dicationic ionic liquid 1,3-bis(3-decylimidazolium-1-yl) propane bromide, and its vapor−liquid interface have been studied using molecular dynamics simulations at room temperature. Starting from a uniform distribution of cations, the system is found to spontaneously evolve forming cross-linked cationic micellar aggregates. Alkyl tails are typically found buried inside the aggregates to minimize their unfavorable interactions with water, whereas the polar head groups are present at the micellar surfaces, exposed to water. Anions are found throughout the solution and are not strongly bound to the cations. Cationic micellar aggregates exhibit an interesting behavior: interconnection mediated by head groups, a phenomenon which is not observed in monocationic ionic liquid solutions. The structure of the vapor−liquid interface of the solution, the structure of the micellar aggregates, and the distribution of counterions are also discussed.

1. Introduction

Room temperature ionic liquids (RTILs) have interesting properties and potential applications.[1−3] Experimental efforts[4−7] and computational studies[8−12] have added to the knowledge on this new class of materials. Binary mixtures are known to possess properties not exhibited by either of the components. The area of applicability of ILs can be enormously increased by mixing them with other compounds and tailoring the mixture for a specific application. Several studies have been carried out in this direction, by mixing ILs with carbon dioxide,[13−15] hydrogen fluoride,[4] water,[16−18] and other compounds.

Aqueous solutions of ionic liquids have been studied extensively using experiments[19−22] and computational techniques,[23,24,16,25,26] the majority of them involving ILs based on imidazolium headgroups. These studies have aided in determining the structure of ILs in solutions. The chain length on the headgroup plays a major role in determining the structure of solutes in the solution. ILs with a small chain on the cation headgroup (≤ 4) remain as monomeric ions in solutions, whereas those with intermediate length chains ($n = 6-8$) form small clusters of cations. When the substituent on the headgroup is long alkyl chain ($n \geq 10$), the cations form micellar aggregates with the alkyl tails buried inside and the head groups lying at the surface.[18,26] Due to the inherent amphiphilic nature of these compounds, they can be used as surfactants.

Geminal dicationic ILs consist of a doubly charged cation that is composed of two singly charged cations linked by an alkyl chain (also called a spacer). A singly charged anion is associated with each of the charged parts of the cation in the crystalline phase. Such ILs with more than one polar and nonpolar region have been synthesized and characterized[27−31] and applied in chemical reactions[32,33] recently. Dicationic and tricationic ILs expand the horizon of applications for ionic liquids.[34−36] Crystal structures of some compounds belonging to this class have also been determined by Anderson et al.[27] ILs are also known to aggregate at very small concentrations and hence are useful as surfactants. A systematic study on monocationic and dicationic imidazolium bromide ILs with a tetradecyl chain has shown that the

* To whom correspondence should be addressed. Phone: +1-215-204-4217. Fax: +1-215-204-2257. E-mail: bhargav@sas.upenn.edu.

† Temple University.

‡ University of Pennsylvania.

10.1021/ct900674t
Published on Web 02/08/2010

dicationic compound is thermally more stable and also possesses a significantly lower CMC (about 200 times less).[28]

Dicationic ILs can be used as solvents and lubricants at high temperatures.[37] They also find applications in analytical chemistry, particularly in electrospray ionization mass spectrometry and in detecting small quantities of anions via gas phase ion association[38] and as the stationary phase in gas chromatography columns.[39] These group of ILs have received very little attention of researchers compared to the monocationic ILs. There are very few experimental studies on these compounds. Computational studies on dicationic ILs are limited to the electronic structure calculations in the gas phase[40] and semiempirical molecular modeling of interactions between ILs and a hydroxylated silicon surface.[41] To date, there seems to have been no efforts to study the microscopic structure of these materials in bulk using computational methods, such as molecular dynamics (MD). Accordingly, the present work looks into the structure and organization of a dicationic IL 1,3-bis(3-decylimidazolium-1-yl) propane bromide (two 1-*n*-decylimidazolium units linked by a $-(C_3H_6)-$ group) in bulk and the vapor/liquid interface of its aqueous solution. Details of the MD simulations are provided in the next section, which is followed by the results obtained and a discussion of these results. We end with the conclusions derived from the computational studies.

2. Methodology and Simulation Details

Classical MD simulations have been carried out on an aqueous solution of 1,3-bis(3-decylimidazolium-1-yl) propane bromide using the LAMMPS code[42] and the all-atom force field model developed by Pádua and co-workers.[43] [In the dicationic IL studied, the two imidazolium rings are connected to each other through a spacer, compared to the single imidazolium ring for which the model has been developed.[43] The residual charge (due to the replacement of the third hydrogen atoms of 3-methyl groups by a methylene group) has been distributed to the hydrogen atoms (+0.125*e* each) of the central methylene group of the spacer.] The simple point charge (SPC) model[44] has been used for water molecules.

A dicationic IL monomer was replicated in three dimensions and water molecules were added randomly to generate the starting configuration. The system was initially simulated in the isothermal−isobaric (constant NPT) ensemble at 1 atm pressure to fix the density. Equilibration at 1 atm pressure leads to a value of 76.86 Å for the edge length of the cubic box. Subsequent MD runs were performed in the canonical ensemble (constant NVT) with a box length derived from constant NPT simulations. The simulated system consisted of 125 cation entities, each with two units of positive charge, 250 bromide ions, and 11 317 water molecules. Three dimensional periodic boundary conditions were used to simulate the bulk behavior. A distance of 13 Å was chosen as the cutoff distance for computing nonbonded interactions. The potential was not shifted at the cutoff. Long range electrostatic interactions[45] were handled using the particle−particle particle-mesh solver (PPPM) with an accuracy of 1 part in 10^5. The equations of motion were integrated with a time step of 0.5 fs using the velocity Verlet algorithm, and SHAKE[46] was used to constrain the stretching and bending

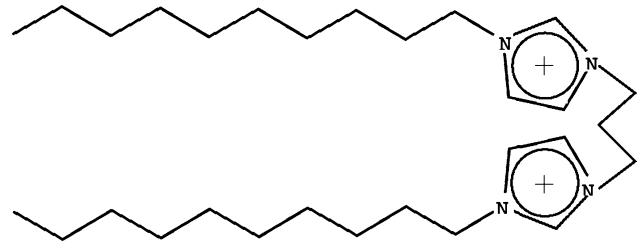

Figure 1. Schematic representation of the cation, 1,3-bis(3-decylimidazolium-1-yl) propane.

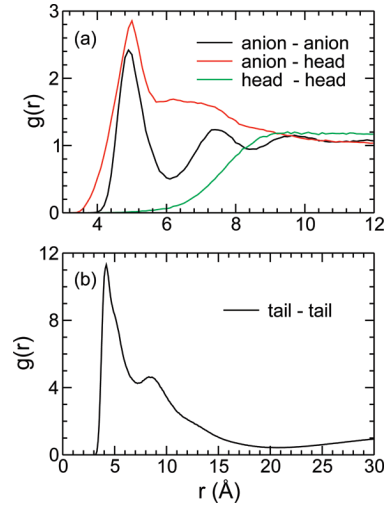

Figure 2. Radial distribution functions (a) between the headgroup and the anion (b) tail groups around themselves.

interactions of water molecules. A Nosé-Hoover thermostat and barostat with time constants of 1000.0 and 500.0 fs were used to control the temperature and pressure of the system, respectively. A trajectory of 40 ns was generated, out of which the final 30 ns was saved for analysis. Positions of the atoms were stored every 4 ps.

A well equilibrated system was placed at the center of a tetragonal box with sides of 76.86, 76.86, and 120.0 Å, to simulate a liquid/vacuum interface. Since the periodic boundary conditions were used on this super cell, the system represented an infinite number of thin films of aqueous IL solution separated by a vacuum. All other conditions remained the same as in the bulk simulations. The system was equilibrated for 10 ns and data for 30 more nanoseconds were saved for analysis.

The visualization software VMD[47] was used to render images of the simulations. A schematic of $[C_3(C_{10}Im)_2]^{2+}$ has been provided as Figure 1 to aid the discussion.

3. Results and Discussion

3.1. Radial Distribution Functions. The average distribution of different types of atoms, without the details of the orientation, can be obtained using pairwise radial distribution functions (RDFs). Different intermolecular RDFs are presented in Figure 2. Data are averaged over the last 10 ns of the trajectory. The center of the imidazolium ring refers to headgroup, and the terminal carbon atom of the decyl chain is referred to as a tail group in the figure. A binwidth of 0.1 Å is used in the calculation of RDFs. From Figure 2a, we

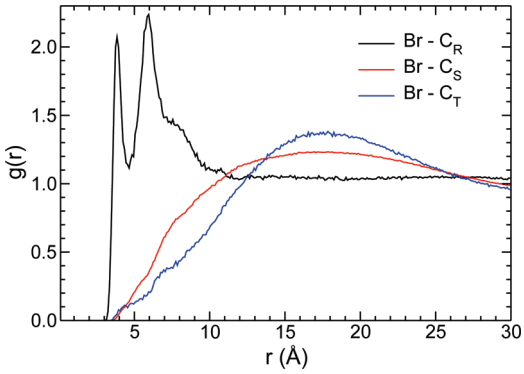

Figure 3. Radial distribution functions of C_R, C_S, and C_T around anions, where C_R's are the carbon atoms present between the two nitrogen atoms of the imidazolium ring, C_S's are the third to ninth carbon atoms of the decyl chain counting from the ring, and C_T's are the terminal carbon atoms of decyl chains.

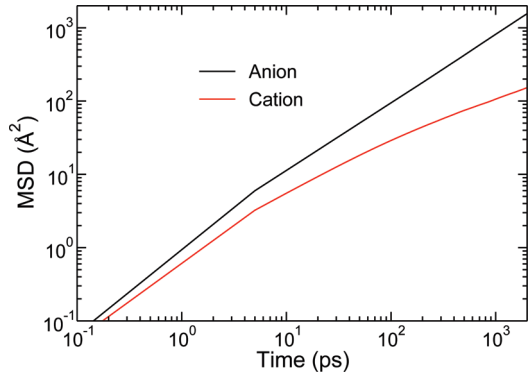

Figure 4. Mean squared displacements of the anion and cation. The data are averaged over the last 10 ns of the trajectory.

can see that the anion is very well organized around the cation. The anion−anion RDF shows a first maximum at 4.9 Å and has a coordination number of 0.43 up to the first minimum at 6.1 Å. The RDF also shows several noticeable maxima before the function attains its isotropic value of unity. The first peak in this function arises from the near neighbor bromide ions, whereas the subsequent peaks arises from the anions which are separated by a single water molecule, two water molecules, and so on. The anion−head RDF shows a sharp peak at 5 Å with an amplitude of 2.8, followed by a broad hump between 5.7 and 8.0 Å. The coordination number up to 8.0 Å is 1.8, which is the average number of head groups found within a distance of 8.0 Å from a particular anion. The RDF does not show any further features beyond 12 Å. The head−head radial distribution function shows a broad peak around 10 Å with an amplitude of 1.2. A broader second peak has been observed at around 24 Å (data not shown). The reason for the appearance of this peak will be discussed later in this section. Figure 2b shows the intermolecular radial distribution between the terminal carbon atoms of the decyl chain. The RDF peaks at 4.2 Å with an amplitude of 11.3, which suggests the extent of organization of decyl chains in the solution. The distribution is similar to that found in monocationic ILs with a long alkyl chain substituted on the ring.[26] The formation of aggregates is evident from the distribution of tail groups around themselves.

The radial distribution of atoms C_R (carbon atom between the two nitrogen atoms in the ring), C_S (third to ninth carbon atoms of decyl chain counting from the ring), and C_T (terminal carbon of decyl chain) around anions are shown in Figure 3. The RDF of C_R around the anion exhibits two sharp peaks at 3.95 and 5.95 Å. The first peak arises from the interaction of anions with the hydrogen attached to C_R. This hydrogen atom has been found to be more acidic compared to the other two hydrogen atoms on the imidazolium ring and form hydrogen bonds with the anion in pure ionic liquids and in IL solutions.[48,26] The second peak arises from the interaction with a second C_R atom present on the connected ring. It is interesting to note that the peaks for the C_S and C_T RDFs around the anion are broad and are present at around 18 Å, suggesting negligible interaction between the alkyl tail and anions. The peak position of the anion−C_T RDF provides an estimate of the median distance of anions from the terminal carbon atom of the decyl chain.

3.2. Hydrogen-Bonded Interactions. Hydrogen bonds (H-bonds) formed in the solution have been determined on the basis of geometric criteria. A hydrogen bond is said to have formed between the atoms if the distance between them is less than the sum of their van der Waals radii and they satisfy the linearity condition. We have chosen the H-bonds with a distance cutoff of 2.7 Å for bonds involving oxygen and 3.0 Å for bonds involving the bromide ion and an angle cutoff of 160° (spread < 20°) as strong H-bonds. We have characterized weak hydrogen bonds by adding 0.3 Å to the distance cutoff and choosing 140° as an angle cutoff. In the aqueous dicationic IL solutions, it has been observed that only 3% of the cations are bound to the anions with strong H-bonds. Including the weak H-bonds, this number increases to around 27%. Cations are also found to be H-bonded to water molecules. One in three cations are strongly bound to water via H-bonded interactions, and if we include the weak interactions it amounts to an average of 2.75 H-bonds per cation. Bromide ions are known to form strong H-bonds with water.[16] Each bromide ion is strongly bound to around 4 water molecules and weakly bound to two more water molecules. Hydrogen atoms of the imidazolium ring show varying degrees of association through H-bonds. While the acidic hydrogen atom (attached to the carbon atom between two nitrogen atoms of the ring) shows the highest affinity to forming H-bonds, the one bonded to the carbon atom linked with the nitrogen atom with a decyl chain shows the least affinity for H-bonds. This can be attributed to the stearic hindrance from the decyl chain.

3.3. Diffusion of Ions. Mean squared displacements (MSD) of the anion and cation are shown in Figure 4. The central carbon atom of the spacer propyl group present between the two imidazolium rings is considered as the cation position. The initial ballistic motion of the ions can be observed. From the figure, we can see that the MSD at 2 ns is around 1600 and 150 Å^2, respectively, for the anion and cation; i.e., the MSD of the anions is an order of magnitude higher than that of the cations. On average, anions are displaced by around 40 Å, whereas cations are displaced by a little above 12 Å. The ions diffuse considerably, and hence we can assume that the phase space is sampled adequately to give proper averages for the properties discussed. Anions

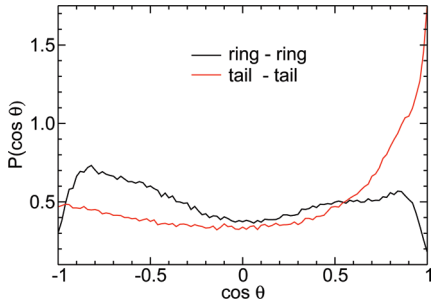

Figure 5. Orientation of polar and nonpolar groups of a cation.

are not strongly bound to cations, which is evident from the higher diffusion rate observed in the case of anions, compared to the cations, even though anions are likely to be found near the acidic hydrogen of the imidazolium ring. The reason for the slow diffusion of cations disproportionate to their mass is discussed later in this section.

3.4. Intramolecular Structure of Cations. The presence of two polar and two nonpolar groups in the cation can lead to a complex intramolecular structure. Both hydrophobic tails of the cation can interact with each other, or they may interact with the hydrophobic tails of another cation. The orientation of the two rings with reference to each other is also influenced by the conformation of the spacer. In Figure 5, the orientation probabilities for the rings and tails are shown: The *x* axis presents the cosine of the angle between two rings (measured as the angle between the normals to the planar rings) and two decyl tails (measured as the angle between the vectors connecting the first and last carbon atom of the decyl tails) belonging to the same cation, and the *y* axis presents the probability. It is clear from the figure that the tails belonging to a cation are likely to be oriented parallel to each other. However, the probabilities for nonparallel orientations are non-negligible. It can also be noticed that there is a higher probability of finding imidazolium rings of a cation oriented around 150° to each other. These are the most likely orientations, and not all the cations have the same intramolecular structure.

3.5. Formation of Aggregates. Cations are found to form aggregates in the aqueous solution in accordance with experimental findings.[28,29] This kind of behavior is also observed in monocationic IL solutions,[17,49,50,26] where the alkyl tails are found to be present at the core of the micellar aggregates. In the case of dicationic ILs, we observe similar behavior but with a difference. The decyl tails interact with each other, thus minimizing their exposure to water, initiating the aggregation process. It is also observed from a partitioning of the energy that the van der Waals interactions between the decyl tails are the main reason for aggregation. The imidazolium head groups surrounding these alkyl groups are thus shielding them from direct interaction with water while at the same time exposing them to favorable interactions. Anions interact with the head groups but are not bound to them strongly. Some of the cations act as linkers between micellar aggregates; i.e., they can be part of two aggregates with each of their decyl chains belonging to different micelles. This kind of interlinking (which is not observed in monocationic ILs[16]) between the aggregates makes the solution very viscous. The peak in the head−head RDF observed at around 24 Å arises from cations belonging to an aggregate and present on the diametrically opposite sides. Also, the observed slow diffusion of cations compared to the anions can be rationalized as due to the formation of interconnected aggregates.

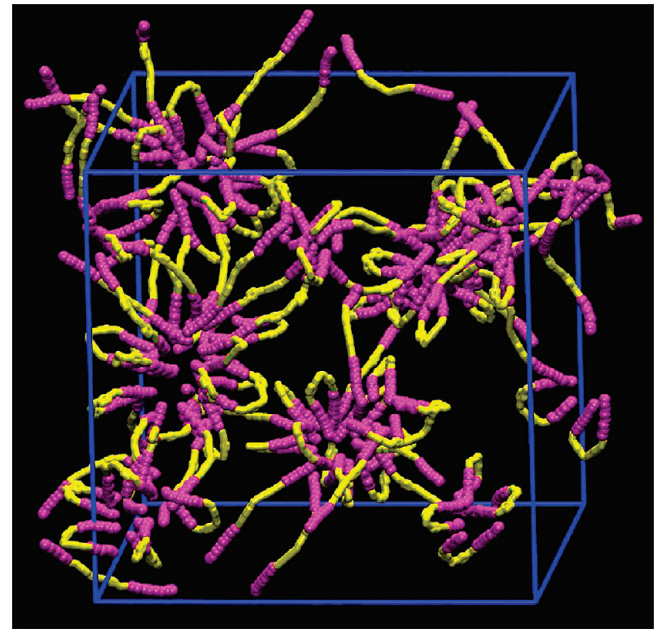

Figure 6. Aggregates of cations in an aqueous solution of $[C_3(C_{10}Im)_2]\cdot 2Br$. The positions are averaged over several frames. The yellow region represents the polar headgroup, while magenta spheres represent atoms belonging to the hydrophobic tail. Hydrogen atoms, anions, and water are not shown for the ease of visualization.

Figure 6 shows the observed aggregation of cations in aqueous solution. In the figure, atoms belonging to the headgroup of the cations are shown in a yellow color, while the atoms belonging to the hydrophobic tail region are shown as magenta spheres. Hydrogen atoms, bromide ions, and water molecules are not shown for clarity. The positions of the atoms are averaged over several frames near the end of the 40 ns simulation. We can notice the formation of near spherical micellar aggregates with the tail region in the core and head groups at the periphery. The links formed between two aggregates through the headgroup are visible in the figure. Anions show some preference to be present near the headgroup but are also found in the regions away from the imidazolium ring (data not shown).

3.6. Structure of an Aggregate. Formation of aggregates in solutions of amphiphilic cations is expected. However, the nature of the aggregates formed in this solution is rather interesting. Unlike those isolated near spherical aggregates formed in the monocationic IL solutions,[16] aggregates with a hydrophobic core and hydrophilic surface interconnected (cross-linked) to each other by the mediating polar region are found in dicationic IL solutions. From Figure 7, we can visualize the hydrophobic region (represented as magenta spheres) in the core of the near spherical aggregate interacting with each other via favorable dispersion interactions. Head groups (represented in yellow) surrounding the hydrophobic part interact with water while shielding the decyl chains from

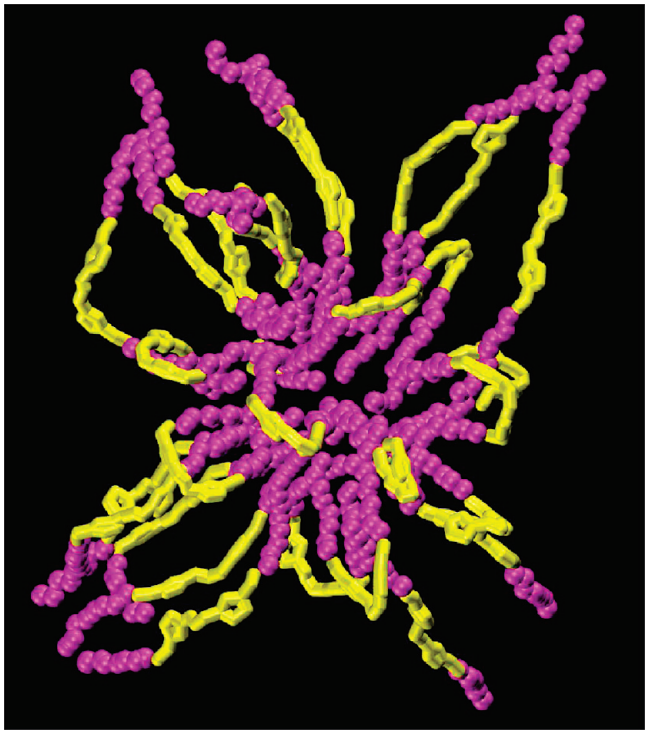

Figure 7. Structure of an aggregate in an aqueous solution of $[C_3(C_{10}Im)_2]\cdot 2Br$. Only the heavy atoms of cations belonging to the aggregate are shown in the figure.

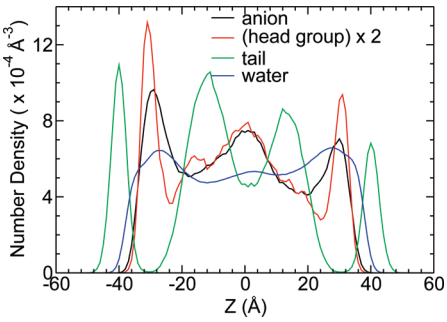

Figure 8. Number density profiles of anions, head groups, tail groups, and water in an aqueous solution of 1,3-bis(3-decylimidazolium-1-yl) propane bromide.

unfavorable exposure to water. Both decyl chains of some cations are involved in the formation of a single micellar aggregate, but others extend outside. In the figure, only one of the aggregate is completely shown, and the decyl chains extending out of the aggregate actually belong to a different aggregate (not shown in the figure).

3.7. Liquid−Vapor Interface. *3.7.1. Number Density.* The number density profiles of anions, head groups, tails, and water along the z axis, obtained from the vapor−liquid interface simulations, are shown in Figure 8. In these calculations, the headgroup is represented by the central carbon atom of the spacer ($-(CH_2)_3-$ group) located between the two imidazolium rings. The terminal carbon atoms of the decyl group represent tail groups. Since the ratio of cations to anions is 1:2 in the solution, we have accordingly multiplied the headgroup number density by two for comparison. Similarly the number density of water is normalized and presented. Notice the peak positions in the number densities of anion and headgroup are close to each other.

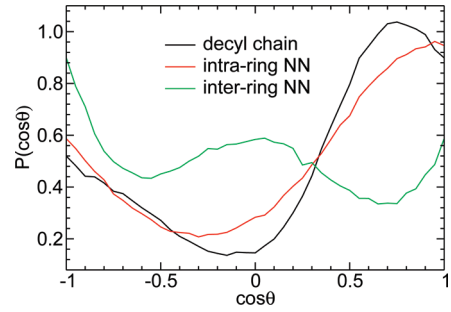

Figure 9. Orientation probability for vectors corresponding to different components of the cation along the z axis. Cos θ is the angle between the z axis and the vectors connecting the (black) first and last carbon atoms of the decyl chain, (red) two nitrogen atoms of an imidazolium ring, and (green) nitrogen atoms connected by the spacer.

However, the peak corresponding to cation is sharp near the interface due to the more organized orientation of cations near the interface. Moreover, the peaks are equally broad for both headgroup and anions in the bulk region of the solution. The reduction in the number density of water in the bulk region can be attributed to the formation of cation aggregates. The number density profile of the tail shows some important characteristics. The tail region is protruding out from the solution interface, which is evident from the profiles of the tail and water. At least some part of the decyl group is completely protruding out from the surface. We can see that the number density of tail groups is highest at the interface and suddenly drops to almost zero. We find two additional peaks in the tail number density in the bulk region of the solution. These peaks, which arise due to the presence of aggregates in the bulk, do not provide much insight, as the data are averaged over the surface. Observing the density profiles of the tail and water, it is obvious that the maxima for water are present near the minima for the tail and vice versa. So the high concentration of tails at a given distance from the interface indicates the formation of aggregates in the solution and hence decreases the available region for the water molecules.

Note the asymmetry present in the density profiles. Asymmetry is generally induced during the initial stages and persists for an extended period of time in the MD simulations. Here, we are only looking at the qualitative behavior of the ions in the aqueous solution. To obtain statistically significant quantitative values, it is advisable to simulate independent configurations and/or bigger systems for longer times.

3.7.2. Orientation of Cation. The orientation probabilities of vectors defining different components of the cation along the z axis are shown in Figure 9. The probabilities are computed only for the cations present beyond a certain cutoff distance from the origin along the z axis. The cutoff distance of 24 Å was chosen on the basis of the number density profile of cations. The probabilities are shown for the vectors connecting the first and last carbon atoms of the decyl chain (black curve), two nitrogen atoms belonging to the same imidazolium ring (red), and nitrogen atoms of different rings connected by the spacer (green). The probability of finding the decyl chain oriented parallel to the surface is the least and is very low (<0.15) compared to the isotropic value of 0.5. The most probable orientation is the chain tilted to the

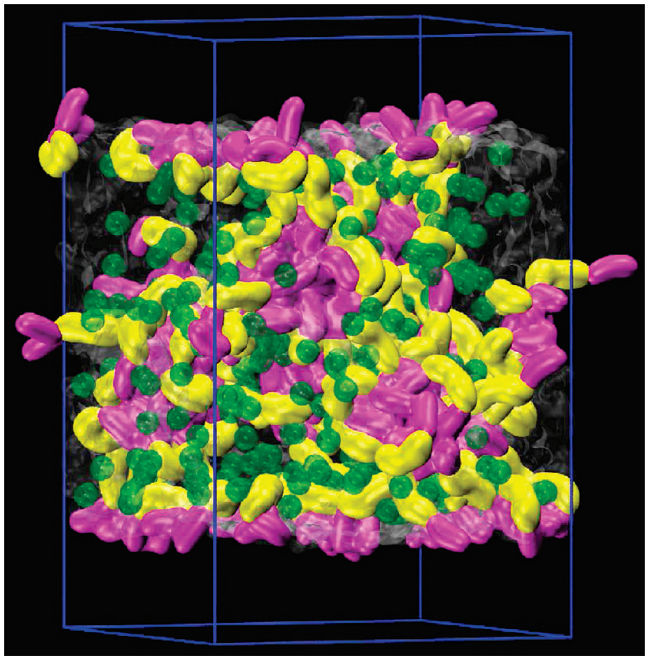

Figure 10. Volume map density of cations, anions, and water in the vapor−liquid interface of an aqueous solution of $[C_3(C_{10}Im)_2]\cdot 2Br$. Yellow represents the polar headgroup region, while magenta represents the hydrophobic tail group. Anion density is shown in green, and the water density is shown in transparent white.

interface normal. There is also a substantial probability of finding the chain oriented parallel to the interface normal. The vector connecting two nitrogen atoms of the ring is likely to be parallel to the interface normal. The orientation probability for the vector connecting nitrogen atoms separated by the spacer shows interesting behavior. We can see the peaks corresponding both to the parallel and perpendicular orientation of this vector with reference to the interface normal. The peak around zero corresponding to the perpendicular orientation arises from the cations that have both decyl chains at the interface parallel to each other, so that the spacer is perpendicular to these chains and hence to the z axis. The peak around 1 (or −1) corresponding to the parallel orientation along the z axis, arises from those cations with a decyl chain at the interface and the other inside the bulk region, belonging to an aggregate.

3.7.3. Organization at the Vapor−Liquid Interface. Observing the density profiles and orientation probability, it is evident that the decyl chains are present at the vapor−liquid interface of the dicationic IL solution partially protruding out of the water surface. These alkyl chains are likely to be tilted to the interface normal. A volume map density of the vapor−liquid interfacial system is presented in Figure 10. No ions were found in the vapor region of the interface. It can be observed from the figure that the segregation of polar and nonpolar regions of the cation that occurs is similar to that found in bulk MD simulations; namely, hydrophobic regions are surrounded by hydrophilic regions. The aggregates formed in the bulk region with decyl chains in the core are connected to each other via mediating head groups of the cations. Anions are found dispersed throughout the available region of the solution excluding the core of the aggregates.

4. Conclusions

The structure and organization in an aqueous solution of a dicationic ionic liquid and its liquid−vapor interface at a concentration higher than critical aggregation concentration (CAC) is studied using MD simulations at room temperature. Starting from a uniform distribution of cations, evolution of the system to form cationic aggregates has been observed. Anions are found to form a well-defined solvation shell of water via hydrogen-bonded interactions. Cationic head groups are also found to form H-bonds with water, though not as strongly as anions. Cations aggregate in such a way as to minimize the unfavorable interactions between the hydrophobic tail groups and water, while maximizing the favorable polar headgroup−water interactions. Thus, the core of the aggregate is devoid of water and anions, populated with only the decyl chains held together by van der Waals attraction. Partitioning of nonbonded interaction energies indicates the tail−tail interactions to be the major reason for the formation of aggregates.

Anions in the solution are present throughout the solution even though they are found to interact with the ring hydrogen atoms. The anions are not strongly bound to cations, which is evident from the diffusion of the ions. Unlike in monocationic aqueous IL solutions,[16] the aggregates in a dicationic IL solution are interconnected (cross-linked) to each other via mediating cations. Some of the cations are shared between two distinct aggregates with each of the head and tail groups belonging to one of them. The interconnection between the aggregates makes the solution highly viscous, which is also reflected in the diffusion of cations. The vapor−liquid interface of the aqueous solution is populated by the decyl chains that partially protrude out of the water surface. The alkyl tails are tilted to interface normal at a small angle. While some of the cations are entirely present in the interfacial region, others share their tails between the interface and the micellar aggregate present in the bulk. Interconnected aggregates are also found in the bulk region of the interfacial system.

In the present studies, MD simulations are performed on a very concentrated solution of 0.457 M, while the CAC values are very small, on the order of millimolar.[29] The current study only addresses the behavior of the solution at a higher concentration, and the structure of the aggregates at CMC may be different than that observed in these simulations. On the basis of the structure of the aggregates in the solution, IL−water mixtures with even higher concentrations of IL are likely to form bilayers of ILs. It will be interesting to see whether such a bilayer is made up of the folded or the extended form of the cation or a mixture of both, and also how they behave with changes in the IL concentration and the length of the spacer. These studies require simulations of large systems to be performed for a long duration of time and are feasible only through coarse-grained methods, with present day computational resources. Thus, it will be advisable to use coarse-grained MD simulations, to build on the present results and also to study the dicationic IL solutions at or near the critical aggregation concentrations.

Acknowledgment. We thank the Ras Al Khaimah Center for Advanced Materials for supporting this work through a research fellowship named for His Highness Sheikh Saqr Bin Mohammed Al Qasimi.

Supporting Information Available: Example LAMMPS input, parameter, and data files. This material is available free of charge via the Internet at http://pubs.acs.org.

References

(1) Tong, J.; Liu, Q.; Xu, W.; Fang, D.; Yang, J. *J. Phys. Chem. B* **2008**, *112*, 4381–4386.

(2) Huddleston, J. G.; Visser, A. E.; Reichert, W. M.; Willauer, H. D.; Broker, G. A.; Rogers, R. D. *Green Chem.* **2001**, *3*, 156–164.

(3) Welton, T. *Chem. Rev.* **1999**, *99*, 2071–2084.

(4) Hagiwara, R.; Hirashige, T.; Tsuda, T.; Ito, Y. *J. Fluorine Chem.* **1999**, *99*, 1–3.

(5) Triolo, A.; Mandanici, A.; Russina, O.; Rodriguez-Mora, V.; Cutroni, M.; Hardacre, C.; Nieuwenhuyzen, M.; Bleif, H.; Keller, L.; Ramos, M. A. *J. Phys. Chem. B* **2006**, *110*, 21357–21364.

(6) Triolo, A.; Russina, O.; Bleif, H.; Di Cola, E. *J. Phys. Chem. B* **2007**, *111*, 4641–4644.

(7) Xiao, D.; Rajian, J. R.; Li, S.; Bartsch, R. A.; Quitevis, E. L. *J. Phys. Chem. B* **2006**, *110*, 16174–16178. Xiao, D.; Rajian, J. R.; Cady, A.; Li, S.; Bartsch, R. A.; Quitevis, E. L. *J. Phys. Chem. B* **2007**, *111*, 4669–4677.

(8) Hanke, C. G.; Price, S. L.; Lynden-Bell, R. M. *Mol. Phys.* **2001**, *99*, 801–809.

(9) Hu, Z.; Margulis, C. J. *Acc. Chem. Res.* **2007**, *40*, 1097–1105.

(10) Bhargava, B. L.; Balasubramanian, S. *J. Phys. Chem. B* **2008**, *112*, 7566–7573.

(11) Maginn, E. J. *J. Phys.: Condens. Matter* **2009**, *21*, 373101.

(12) Annapureddy, H. V. R.; Hu, Z.; Xia, J.; Margulis, C. J. *J. Phys. Chem. B* **2008**, *112*, 1770–1776.

(13) Huang, X.; Margulis, C. J.; Li, Y.; Berne, B. J. *J. Am. Chem. Soc.* **2005**, *127*, 17842–17851.

(14) Bhargava, B. L.; Krishna, A. C.; Balasubramanian, S. *AIChE J.* **2008**, *54*, 2971–2978.

(15) Shi, W.; Maginn, E. J. *J. Phys. Chem. B* **2008**, *112*, 2045–2055.

(16) Bhargava, B. L.; Klein, M. L. *J. Phys. Chem. A* **2009**, *113*, 1898–1904.

(17) Blesic, M.; Marques, M. H.; Plechkova, N. V.; Seddon, K. R.; Rebelo, L. P. N.; Lopes, A. *Green Chem.* **2007**, *9*, 481–490.

(18) Bhargava, B. L.; Klein, M. L. *Soft. Matter* **2009**, *5*, 3475–3480.

(19) Firestone, M. A.; Dzielawa, J. A.; Zapol, P.; Curtiss, L. A.; Seifert, S.; Dietz, M. L. *Langmuir* **2002**, *18*, 7258–7260.

(20) Zhang, H.; Liang, H.; Wang, J.; Li, K. *Z. Phys. Chem.* **2007**, *221*, 1061–1074.

(21) Zhao, Y.; Gao, S.; Wang, J.; Tang, J. *J. Phys. Chem. B* **2008**, *112*, 2031–2039.

(22) Blesic, M.; Lopes, A.; Melo, E.; Petrovski, Z.; Plechkova, N. V.; Lopes, J. N. C.; Seddon, K. R.; Rebelo, L. P. N. *J. Phys. Chem. B* **2008**, *112*, 8645–8650.

(23) Jiang, W.; Wang, Y.; Voth, G. A. *J. Phys. Chem. B* **2007**, *111*, 4812–4818.

(24) Wang, Y.; Jiang, W.; Yan, T.; Voth, G. A. *Acc. Chem. Res.* **2007**, *40*, 1193–1199.

(25) Bhargava, B. L.; Klein, M. L. *Mol. Phys.* **2009**, *107*, 393–401.

(26) Bhargava, B. L.; Klein, M. L. *J. Phys. Chem. B* **2009**, *113*, 9499–9505.

(27) Anderson, J. L.; Ding, R.; Ellern, A.; Armstrong, D. W. *J. Am. Chem. Soc.* **2005**, *127*, 593–604.

(28) Ding, Y.; Zha, M.; Zhang, J.; Wang, S. *Colloids Surf., A* **2007**, *298*, 201–205.

(29) Baltazar, Q. Q.; Chandawalla, J.; Sawyer, K.; Anderson, J. L. *Colloids Surf., A* **2007**, *302*, 150–156.

(30) Liu, X.; Xiao, L.; Wu, H.; Chen, J.; Xia, C. *Helv. Chim. Acta* **2009**, *92*, 1014–1021.

(31) Lovelock, K. R. J.; Deyko, A.; Corfield, J.-A.; Gooden, P. N.; Licence, P.; Jones, R. G. *ChemPhysChem* **2009**, *10*, 337–340.

(32) Han, X.; Armstrong, D. W. *Org. Lett.* **2005**, *7*, 4205–4208.

(33) Liu, Q.; van Rantwijk, F.; Sheldon, R. A. *J. Chem. Technol. Biotechnol.* **2006**, *81*, 401–405.

(34) Zhang, Z. X.; Zhou, H. Y.; Yang, L.; Tachibana, K.; Kamijima, K.; Xu, J. *Electrochim. Acta* **2008**, *53*, 4833–4838.

(35) Zafer, C.; Ocakoglu, K.; Ozsoy, C.; Icli, S. *Electrochim. Acta* **2009**, *54*, 5709–5714.

(36) Li, X.; Bruce, D. W.; Shreeve, J. M. *J. Mater. Chem.* **2009**, *19*, 8232–8238.

(37) Jin, C.; Ye, C.; Phillips, B. S.; Zabinski, J. S.; Liu, X.; Liu, W.; Shreeve, J. M. *J. Mater. Chem.* **2006**, *16*, 1529–1535.

(38) Nachtigall, F. M.; Corilo, Y. E.; Cassol, C. C.; Ebeling, G.; Morgon, N. H.; Dupont, J.; Eberlin, M. N. *Angew. Chem., Int. Ed.* **2008**, *47*, 151–154.

(39) Han, X.; Armstrong, D. W. *Acc. Chem. Res.* **2007**, *40*, 1079–1086.

(40) Sun, H.; Zhang, D.; Liu, C.; Zhang, C. *THEOCHEM* **2009**, *900*, 37–43.

(41) Nooruddin, N. S.; Wahlbeck, P. G.; Carper, W. R. *Tribol. Lett.* **2009**, *36*, 147–156.

(42) Plimpton, S. J. *J. Comput. Phys.* **1995**, *117*, 1–19; [Online] http://lammps.sandia.gov.

(43) Lopes, J. N. C.; Deschamps, J.; Pádua, A. A. H. *J. Phys. Chem. B* **2004**, *108*, 2038–2047. *108*, 11250;Lopes, J. N. C.; Pádua, A. A. H. *J. Phys. Chem. B* **2006**, *110*, 19586–19592.

(44) Berendsen, H. J. C.; Postma, J. P. M.; van Gunsteren, W. F.; Hermans, J. In *Intermolecular Forces*; Pullman, B., Ed.; Reidel: Dordrecht, 1981; p331−342.

(45) Allen, M. P.; Tildesley, D. J. *In Computer Simulation of Liquids*; Clarendon: Oxford, 1987.

(46) Ryckaert, J. P.; Ciccotti, G.; Berendsen, H. J. C. *J. Comput. Phys.* **1977**, *23*, 327–341.

(47) Humphrey, W.; Dalke, A.; Schulten, K. *J. Mol. Graphics* **1996**, *14*, 33–38.

(48) Del Popolo, M. G.; Lynden-Bell, R. M.; Kohanoff, J. *J. Phys. Chem. B* **2005**, *109*, 5895–5902.

(49) Inoue, T.; Dong, B.; Zheng, L. *J. Colloid Interface Sci.* **2007**, *307*, 578–581.

(50) Vanyúr, R.; Biczók, L.; Miskolczy, Z. *Colloids Surf., A* **2007**, *299*, 256–261.

CT900674T